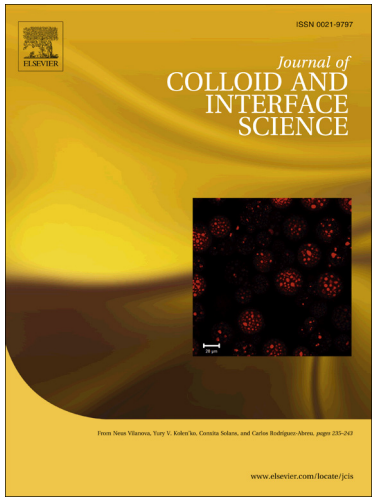

Synthesis and Stability of IR-820 and FITC Doped Silica Nanoparticles

Atul V. Thorat, Tandra Ghoshal, Lan Chen, Justin D. Holmes, Michael A. Morris

PII: S0021-9797(16)30932-8
DOI: http://dx.doi.org/10.1016/j.jcis.2016.11.055
Reference: YJCIS 21783

To appear in: *Journal of Colloid and Interface Science*

Received Date: 14 July 2016
Revised Date: 14 November 2016
Accepted Date: 15 November 2016

Please cite this article as: A.V. Thorat, T. Ghoshal, L. Chen, J.D. Holmes, M.A. Morris, Synthesis and Stability of IR-820 and FITC Doped Silica Nanoparticles, *Journal of Colloid and Interface Science* (2016), doi: http://dx.doi.org/10.1016/j.jcis.2016.11.055

Synthesis and Stability of IR-820 and FITC Doped Silica Nanoparticles

Atul V. Thorat,[1,2] Tandra Ghoshal,[1,2] Lan Chen,[3] Justin D. Holmes,[1,2] and Michael A. Morris[1*]

[1]Surface and Interface Engineering, Advanced Materials and BioEngineering Research (AMBER), Trinity College Dublin, Dublin, Ireland

[2]Department of Chemistry and Tyndall National Institute, University College Cork, Cork, Ireland

[3]National Centre for Nanoscience and Technology, Beijing, China

[*] Corresponding Author: Prof. Michael A. Morris

E-mail: morrism2@tcd.ie

Tel: +353 1 896 3089

Abstract

Fluorescent silica nanoparticles (NPs) have potential in biomedical applications as diagnostics and traceable drug delivery agents. In this study, we have synthesized fluorescent dye grafted silica NPs in two step process. First, a stable method to synthesize various sizes of silica NPs ranging from 20 to 52, 95, 210 and 410 nm have been successfully demonstrated. Secondly, as-synthesized silica NPs are readily grafted with some fluorescent dyes like IR-820 and fluorescein isothiocyanate (FITC) dyes by simple impregnation method. IR-820 and FITC dyes are 'activated' by (3-mercaptopropyl)trimethoxysilane (MPTMS) and (3-aminopropyl)triethoxysilane (APTS) respectively prior to the grafting on silica NPs. UV-Vis spectroscopy is used to test the stability of dye grafted silica NPs. The fluorescent dye grafted silica NPs are quite stable in aqueous solution. Also, a new type of dual dye-doped hybrid silica nanoparticles has been developed. The combination of microscopic and spectroscopic techniques shows that the synthesis parameters have significant effects on the particle shape and size and is tuneable from a few nanometers to a few hundred nanometers. The ability to create size controlled nanoparticles with associated (optical) functionality may have significant importance in bio-medical imaging.

1. Introduction

Monodispersed nanometer-sized particles were shown the importance and advantages in the scientific field as well as in the industrial applications, e.g. catalysis, drug delivery, biolabelling, pharmacy, etc [1-3]. Of these particles, silica NPs are used to make electronic substrates, thin film substrates, electrical insulators, thermal insulators and humidity sensors [4, 5]. Silica NPs also have biomedical applications such as delivery of anticancer drugs [6], enzymes [7] and DNA [8]. The silica NPs play a different role in different systems as these NPs are highly hydrophilic and easy to prepare, separate and label.

Dye doped fluorescent silica NPs (FSNP) possess several advantages like high florescence intensity, good photostability [9, 10] and good potential for surface modification with various biomolecules [11, 12]. During the synthesis, when the dye molecules are doped inside the silica matrix as well as on the surface which protects the dye from the surrounding environment improving their probe sensitivity. FSNP synthesis is relatively simple and does not require extreme reaction conditions such as high/low temperature, pressures and inert reaction environment. Generally, florescent dye molecules are introduced into silica NPs by amino-terminated alkyltrialkoxysilane compounds such as (3-aminopropyl) triethoxysilane (APTS) and dye molecules with an isothiocyanate functional group [13]. The silica surface makes these silica NPs chemically inert and physically stable [14]. This can allow ‘targeting’ of functionality on particular cell types. In addition, these NPs can be biofunctionalized with a wide array of different molecular recognition probes, such as antibodies or aptamers [15]. Single dye-doped silica NPs have previously been used for ultrasensitive DNA analysis down to sub-fmol/L concentrations [16]. Each nanoparticle encapsulates hundreds or even thousands of dye molecules in a ~60 nm silica sphere [15]. Therefore, even considering the likely quenching between the closely packed molecules inside the matrix, an overall fluorescence between two and three orders of magnitude larger than that from individual dyes

is usually achieved, thus providing an extremely strong fluorescence signal for ultrasensitive bioanalysis.

A great many methods have been reported for the preparation of silica NPs, including plasma synthesis [17], chemical vapour deposition (CVD) [18], sol–gel processing [19, 20], chemical precipitation [21], microemulsion processing [22], combustion synthesis [23], continuous microwave hydrothermal technique [24] and pressurized carbonation [25]. Many years ago, Stöber et al [26]. reported a sol-gel method for preparation of monodisperse spherical silica particles, by hydrolysis of tetraethyl orthosilicate (TEOS), in ethanolic medium in the presence of ammonia. In order to prepare uniform-sized spherical particles with wide size range, it is essential to separate nucleation and growth processes, which basically correlate with monodispersity of products. In this work, silica NPs were prepared by modifying Stöber method. This method has advantages in that it does not require extreme conditions of temperature and pressure and the particle size and shape was simply controlled by varying the base concentration.

Herein, we have successfully synthesized monodispersed silica NPs with a size range of 20-400 nm using Stöber method, showing its flexibility for the fabrication of different sizes of silica nanoparticles. Two different dyes (IR-820 and FITC) were successfully grafted on silica surfaces and stability of these dye grafted silica NPs is studied using UV-Vis spectroscopy. Also, a new type of dual dye grafted hybrid silica NPs has been developed. The combination use of TEM, SEM, UV-Vis and confocal microscope shows the synthesis parameters have significant effects on the particle shape and size and the size is tuneable from few nanometers to few hundred nanometers. The ability to create size controlled NPs with associated (optical) functionality have significant importance in bio-medical imaging.

2. Experimental section:

2.1. Materials

IR-820, fluorescein isothiocyanate (FITC), tetraethyl orthosilicate (TEOS, 99.999%), (3-aminopropyl)triethoxysilane (APTS), tert-butyl methyl ether (TBME), dimethyl formamide (DMF), (3-mercaptopropyl)trimethoxysilane (MPTMS), anhydrous ethanol (≥99.9%), 28% aqueous ammonia and toluene were obtained from Sigma-Aldrich and used as received.

2.2. Synthesis of silica NPs

Various sized monodisperse silica NPs were prepared by hydrolysis and then condensation (polymerisation) of TEOS. 0.37 M of TEOS was added into 50 ml of anhydrous ethanol with stirring forming solution 'A'. In another bottle, given volume (weight) of ammonia was mixed with 50 ml anhydrous ethanol to form solution 'B'. Then, solution 'A' was poured into 'B' under rigorous stirring. The mixed solution was kept stirring at room temperature for 24 h. The final molar ratio of TEOS:water:NH_3:ethanol was variable and set to 1:(3.41-12.55):(1.77-6.54):17.13. Finally, the white precipitates were collected by filtration on a piece of Millipore filter paper (pore size ranges from 0.015 – 0.2 μm) followed by washing with ethanol and acetone. Samples were dried under vacuum at room temperature. In order to investigate the effects of the chemical composition in the starting solution on the particle size, amount of the aqueous ammonia was varied. In each case, TEOS:ethanol ratio was fixed.

2.3. Synthesis of IR820-MPTMS and FITC-APTS conjugates

IR-820 (0.6 mM), anhydrous DMF (0.1 M), MPTMS (0.7 mM) and triethyl amine (0.7 mM) were mixed together and stirred for 24 h at room temperature. Then conjugated dye was precipitated by TBME. The 'wet' product was collected by filtration and washed three times using TBME. Sample was dried in vacuum at room temperature. Similarly, FITC (0.8 mM) dye was added to the APTS (10 mM). The access of APTS was added to FITC to prevent bleaching of the dye. The mixture was stirred for 48 h at room temperature. Then this

mixture was precipitated by TBME and sonicated for 20 min. The product was collected by centrifugation at 8000 rpm for 15 min followed by washing with TBME. Then the conjugate was dried under vacuum at room temperature.

2.4. Synthesis of dye grafted silica NPs

A simple imposition method was used to prepare dye grafted silica NPs. As prepared different sizes of silica NPs (0.1 g) were mixed with toluene and then sonicated for 20 min. IR820-MPTMS dye conjugate (0.005-0.05 g) was then added to that solution. These mixtures were then refluxed at 120 °C for 12 h. The solutions were filtered using Millipore filter paper and washed several times with ethanol, water and acetone. All samples were dried under vacuum at room temperature. Similarly, FITC-APTS conjugate (0.025-0.05 g) was added to sonicated solutions of as synthesized different sizes of silica NPs and toluene. Mixtures were refluxed at 120 °C for 12 h. The solutions were filtered using Millipore filter paper and washed several times with ethanol, water and acetone. All samples were dried under vacuum at room temperature.

2.5. Synthesis of dual dye grafted hybrid silica NPs

0.1 g of silica NPs (SiN95) were mixed with toluene and sonicated for 20 min. IR820-MPTMS dye conjugate (0.005 g) was added to the above solution and then refluxed at 120 °C for 12 h. The solution was filtered using filter paper and the solid recovered washed several times with ethanol and water. The sample was dried under vacuum at room temperature. Resultant IR820-MPTMS grafted silica NPs were again dispersed in toluene and sonicated for 20 min. The FITC-APTS dye conjugate (0.01g in 5 ml of toluene) was added to above solution and refluxed at 120 °C for 12 h. The solution was filtered using filter paper and washed several times with ethanol and water. The sample was dried under vacuum at room temperature.

2.5. Characterization

The particle size of silica NPs was analysed by using transmission electron microscope (TEM) and scanning electron microscope (SEM). TEM images were recorded using a JEOL 2010 microscope operated at a voltage of 200 kV. TEM samples were prepared by placing a drop of silica NPs solution (in ethanol) directly onto the carbon-coated copper grid (400 mesh). SEM images were taken from a FEI inspect SEM microscope where the samples were spun coated on a piece of silicon wafer. UV-Vis absorbance spectra were collected by a Cary 50 UV-Visible spectrophotometer. Photoemission steady state spectra were acquired by a Perkin Elmer LS 50 B spectrometer. Fluorescent images were obtained by an Olympus FluoView FV1000 confocal laser scanning microscope working under a Multi Ar laser (458, 488, 514 nm) and a red HeNe laser (633 nm).

3. Results and Discussions

3.1. Morphological characterization of silica NPs by SEM and TEM

One of the main aims of our work was to optimise the size of silica NPs during the synthesis. For potential biomedical applications silica NPs of small sizes are required. The most important parameters involved in the production of these particles are the quantities of the reagents i.e. TEOS, ethanol, water and ammonia solution. Varying each of these parameters one at a time would be inefficient and time consuming. Herein, monodispersed spherical silica NPs with the size ranging from 20 to 52, 95, 210 and 410 nm were successfully prepared by controlled hydrolysis of TEOS in ethanol and varying the ratio of the base to the silica precursor.

It was found that the particle size gradually increased when the added amount of ammonium hydroxide was increased. This may be seen counter initiative as it would be experienced that the number of nuclei per unit volume in the reaction increases with increasing the amount of ammonium hydroxide. However, ammonium hydroxide is the base

catalyst for the hydrolysis as well as for the condensation of TEOS resulting in faster kinetics and consequently larger particle sizes [27].

In Table 1, the experimental variation in ingredients is shown. In Figure 1 and Figure 3 indicative results of SEM and TEM analysis are provided respectively. The images revels that the particle size was increased as the ratio of NH_3:TEOS increased from 2.22 to 8.86. Figure 4 shows the plot of particle size against the NH_3:TEOS ratio. Particle size distributions obtained from SEM images of the silica NPs are shown in Figure 2 and indicate particles of good size monodispersivity. As can be seen in the figures and Table 1, the particle diameter of synthesized silica NPs could be controllably varies from 20 nm to 410 nm without significant increase in the particle size distribution. As shown in TEM micrographs (Figure 3), the silica NPs showed a uniform spherical shape especially for the larger particles. This contrasts the SEM results which appeared to indicate almost polyhedral shapes (Figure 1) but this might be due to higher TEM resolutions.

The surface area and porosity of the silica NPs were characterized by nitrogen adsorption (Table 2). As can be seen in the table, as size increases the surface area and pore size decreases according to BET. The decrease in surface area is as expected from geometrical considerations.

If we assume that the number of particles in 1 g of a powder are:

$$\frac{1}{\frac{4}{3}(\pi r^3 p)} \qquad \text{Eq. 1}$$

where, p = density, r = radius of the particles. The surface area of 1 g of particles is given by:

$$4\pi r^2 \times \frac{1}{\frac{4}{3}(\pi r^3 p)} \qquad \text{Eq. 2}$$

Thus, the surface area of 1 g of particles can be estimated as:

$$\frac{3}{pr} \times 10^3 \qquad \text{Eq. 3}$$

This assumes the particles are dense and have a bulk density of 2.65 g cm^{-2}. The calculated (shown in brackets) and measured surface area of the particles is shown in Table 2. The data are in good agreement suggesting that the particles are essentially non-porous in nature. This is supported by the SEM and TEM images that give little indication of pores. Since these might be expected due to increase in the surface area considerably. The calculated surface areas are somewhat higher for smaller particle sizes but this might be related to the slower growth kinetics allows some nuclei aggregation and resulting in trapped pore volume. This is indicated by the decrease in pore volume with increasing particle size. The decrease in pore size noted probably reflects only the packing of the particles and is related to the pore structure formed between the particles. As size increases, the particles became more regular in size and pack more densely and efficiently decreasing the effective pore size.

It proved exceptionally difficult to monitor the coverage of the dyes trapped in the pores structure formed between particles. Physical methods such as x-ray photoelectron spectroscopy did not properly assess material on the inner pore structures between particles and elemental analysis proved inaccurate. Further, data proved inconsistent if dried materials were placed insolvent and the dye re-dissolved (presumably due to strength of the bond). Instead, we used conditions where we would expect monolayer adsorption was present on the samples produced here. This was a result of a series of adsorption isotherms which revealed monolayer adsorption after 4-8 h (at the solution concentrations used) using Langmuir kinetics. For all materials the adsorption times used were higher than this. E.g. the monolayer saturation value (per g of silica) was estimated at 0.033 g for FITC on SiN52. This is equivalent to 5 x10^{19} molecules on 64 m^2 g^{-1} of the silica or a topological surface are of 1.25 nm^2 which is in agreement with known values [28].

3.2. Functionalization of silica NPs with fluorescent dyes

An extensive review of the synthesis procedures and methods for surface modification of fluorescent silica NPs has been presented earlier [11, 29]. A wide variety of organic dye molecules, magnetic NPs and luminescent quantum dots can be incorporated into the silica NPs [30, 31]. The dyes can be added directly during the growth of the NPs so that dyes can be simply physically entrapped in the structure, or previously synthesized silica NPs to enable its covalent binding to the silica matrix. We have used the second method to overcome dye leakage problem. To prevent dye leakage, we have performed an initial preconjugation of the dyes with an organosilane which incorporates an appropriate functional group [32]. To improve photostability of dye grafted silica NPs, dye molecules should be well protected from oxygenated environment. Otherwise, photodegradation of dye molecules would occur in presence of oxygen molecules [33]. Thus, we prepared the fluorescent silica NPs through a two-step process. In the first step, dyes were covalently attached the coupling agent and in the second step, these activated fluorescent dye conjugates were attached to as synthesized silica NPs by imposition of the dyes on the silica network via the formation of covalent bonds between the dye conjugates and a silane group of silica NPs [34-36].

Firstly, the dye IR-820 was covalently attached to the coupling agent MPTMS in presence of DMF and triethylamine (Scheme S1, See Supporting Information). Great care was used to exclude any water from the process in order to prevent hydrolysis and condensation of the MPTMS molecules. This activated IR820-MPTMS conjugate was attached to as synthesized silica NPs (SiN95) by simple impregnation method (Scheme S2, See Supporting Information) by simple imposition method. Once the dye molecules were trapped at the surface of the silica matrix, the NPs were washed with acetone and water to remove any weakly attached materials. Samples were centrifuged to separate the dye grafted NPs from the supernate that might contain free dye molecules that leached out from the particles during synthesis.

Scheme S3 (See Supporting Information) shows the nucleophilic addition reaction of FITC and APTS. The amine group of silane coupling agent (APTS) reacts with the isothiocyanate group of FITC [32] to form N-1-(3-triethoxysilylpropyl)-N-fluoresceinyl thiourea. It showed a nucleophilic addition between the FITC and APTS. The amino group of APTS attacked the thioisocyanate group of FITC, which forms the Schiff base [37]. Water was excluded from this reaction to prevent hydrolysis and condensation of the APTS molecules. This activated FITC-APTS conjugate was attached to as synthesized silica NPs (SiN95) by simple imposition method (Scheme S4, See Supporting Information). These dye grafted silica NPs also washed with water and acetone and centrifuged to remove free dye molecules that leached out from particles.

3.3. Stability of dye grafted silica NPs

To investigate the stability of the dye grafted silica NPs, 0.01 g of dye grafted silica NPs of different nanoparticle sizes were dispersed in 10 ml of ethanol. The UV-Vis spectroscopy is used to determine the stability of the dye grafted silica NPs over the different aging time. The UV-Vis absorbance spectra of the dispersed dye grafted silica NPs solution showed changes in the absorbed intensity after different aging time viz. 0 min, 4 h, 24 h, 4 days, 8 days and 1 month. Figure 5 and Figure 6 shows the UV-Vis absorbance spectra for IR-820 and FITC grafted silica NPs respectively. A clear zero-sum increase-decrease relation of the absorbance intensity at 366 nm and 750 nm for IR820 grafted silica NPs has been observed. The decrease at 750 nm indicates the degradation of the IR-820 dye molecules in aqueous solution while the increase at 366 nm implies the formation of some new absorbers possibly due to intermolecular reactions.

However, the feature absorbance peak of FITC at 490 nm is constant for all FITC grafted silica NPs (Figure 6) indicating the FITC grafted silica NPs are more stable than the IR-820 grafted silica NPs under the same conditions. The FITC dye

has excitation and emission spectrum peak wavelengths of approximately 495 nm and 521 nm. The excitation spectra of FITC grafted silica NPs showed a peak at 492.3 nm and the emission spectra of FITC grafted silica NPs showed the peak at 518.6 nm when excited at 450 nm as shown in Figure 7. The excitation spectrum generally is identical to the absorption spectrum as the fluorescence intensity is proportional to the absorption.

3.4. Dual dye grafted hybrid silica NPs (FITC- IR820-SiO_2)

The fabrication of the FITC-IR820-SiO_2 NPs was carried out by three steps: the synthesis of bare silica NPs with tuneable size; the modification of dyes by reactive silanes and the graft of the bare NPs by the modified dyes. The schematic representation for grafted IR-820 and FITC dyes on silica NPs (SiN95) are shown in Scheme S5 (See Supporting Information). The UV-Vis absorbance spectra (Figure 8) show the presence of both IR-820 and FITC dyes in the silica NPs (SiN95). The peak at 495 nm is due to FITC dye and peak at 840 nm is due to IR-820 dye. Figure 9 shows SEM and TEM image of duel dye grafted silica NPs. This confirms that both the dyes are well incorporated at the surface of the silica NPs. Multiple dye-doped NIR emitting silica NPs are suitable for both time domain optical imaging and multiparametric flow cytometry analyses [38].

3.5. Confocal laser scanning microscopic study of dual dye grafted silica NPs

The novel fluorescent silica NPs not only showed promise for material science but also could lead to a new class of fluorescence probes in biological imaging. The incorporation of dyes into silica matrix was observed by using confocal laser scanning microscopy. Figure 8 shows that confocal laser scanning microscope images of dual dye grafted silica NPs have excellent solubility and stability in water, ethanol and acetonitrile. Figure 10 clearly showed that the dye grafted silica had a strong green fluorescence when they excited at 488 nm and strong red fluorescence when they excited at 633 nm laser light.

The synthesized fluorescent silica NPs could be easily functionalized with different groups [39], so it could also be further conjugated with a variety of biospecies.

4. Conclusion

In this study, we have established a stable method to synthesize fluorescent dye-doped silica nanoparticles with different particle sizes. The method is relatively inexpensive. The combination use of TEM, SEM and UV-Vis shows the synthesis parameters have significant effects on the particle shape and size and the size is tuneable from a few nanometers to a few hundred nanometers. Also, a new type of dual dye-doped hybrid silica nanoparticles has been developed. Confocal microscope images of dual dy doped sample shows flurosence when excited at 488 and 633 nm.

Appendix A. Supplementary material

Supplementary data associated with this article can be found, in the online version, at http:// www.elsevier.com

References:

[1] G. Herbert, Synthesis of monodispersed silica powders II. Controlled growth reaction and continuous production process, J. Eur. Ceram. Soc. 14 (1994) 205-214.

[2] M. Tan, Z. Ye, G. Wang, J. Yuan, Preparation and Time-Resolved Fluorometric Application of Luminescent Europium Nanoparticles, Chem. Mater. 16 (2004) 2494-2498.

[3] C. Kneuer, M. Sameti, U. Bakowsky, T. Schiestel, H. Schirra, H. Schmidt, C.-M. Lehr, A Nonviral DNA Delivery System Based on Surface Modified Silica-Nanoparticles Can Efficiently Transfect Cells in Vitro, Bioconjugate Chem. 11 (2000) 926-932.

[4] S. Coe, W.K. Woo, M. Bawendi, V. Bulovic, Electroluminescence from single monolayers of nanocrystals in molecular organic devices, Nature 420 (2002) 800-803.

[5] T. Tsutsui, Applied physics - A light-emitting sandwich filling, Nature 420 (2002) 752-755.

[6] J. Lu, M. Liong, J.I. Zink, F. Tamanoi, Mesoporous silica nanoparticles as a delivery system for hydrophobic anticancer drugs, Small 3 (2007) 1341-1346.

[7] I.I. Slowing, B.G. Trewyn, V.S.Y. Lin, Mesoporous silica nanoparticles for intracellular delivery of membrane-impermeable proteins, J. Am. Chem. Soc. 129 (2007) 8845-8849.

[8] F. Torney, B.G. Trewyn, V.S.Y. Lin, K. Wang, Mesoporous silica nanoparticles deliver DNA and chemicals into plants, Nat. Nanotechnol. 2 (2007) 295-300.

[9] T. Deng, J.-S. Li, J.-H. Jiang, G.-L. Shen, R.-Q. Yu, Preparation of near-IR fluorescent nanoparticles for fluorescence-anisotropy-based immunoagglutination assay in whole blood, Adv. Funct. Mater. 16 (2006) 2147-2155.

[10] R. Kumar, T.Y. Ohulchanskyy, I. Roy, S.K. Gupta, C. Borek, M.E. Thompson, P.N. Prasad, Near-Infrared Phosphorescent Polymeric Nanomicelles: Efficient Optical Probes for Tumor Imaging and Detection, Acs Appl Mater Inter 1 (2009) 1474-1481.

[11] W.H. Tan, K.M. Wang, X.X. He, X.J. Zhao, T. Drake, L. Wang, R.P. Bagwe, Bionanotechnology based on silica nanoparticles, Med. Res. Rev. 24 (2004) 621-638.

[12] G. Yao, L. Wang, Y. Wu, J. Smith, J. Xu, W. Zhao, E. Lee, W. Tan, FloDots: luminescent nanoparticles, Anal. Bioanal. Chem. 385 (2006) 518-524.

[13] S.W. Ha, C.E. Camalier, G.R. Beck, J.K. Lee, New method to prepare very stable and biocompatible fluorescent silica nanoparticles, Chem. Commun. (2009) 2881-2883.

[14] J.E. Smith, L. Wang, W. Tan, Bioconjugated silica-coated nanoparticles for bioseparation and bioanalysis, Trac-Trends in Analytical Chemistry 25 (2006) 848-855.

[15] M.C. Estevez, M.B. O'Donoghue, X.L. Chen, W.H. Tan, Highly Fluorescent Dye-Doped Silica Nanoparticles Increase Flow Cytometry Sensitivity for Cancer Cell Monitoring, Nano Research 2 (2009) 448-461.

[16] B.A. Holm, E.J. Bergey, T. De, D.J. Rodman, R. Kapoor, L. Levy, C.S. Friend, P.N. Prasad, Nanotechnology in biomedical applications, Mol. Cryst. Liq. Cryst. 374 (2002) 589-598.

[17] A. Bapat, C. Anderson, C.R. Perrey, C.B. Carter, S.A. Campbell, U. Kortshagen, Plasma synthesis of single-crystal silicon nanoparticles for novel electronic device applications, Plasma Phys. Controlled Fusion 46 (2004) B97-B109.

[18] N. Awaji, S. Ohkubo, T. Nakanishi, T. Aoyama, Y. Sugita, K. Takasaki, S. Komiya, Thermal oxide growth at chemical vapor deposited SiO[sub 2]/Si interface during annealing evaluated by difference x-ray reflectivity, Appl. Phys. Lett. 71 (1997) 1954-1956.

[19] B.G. Trewyn, I.I. Slowing, S. Giri, H.-T. Chen, V.S.Y. Lin, Synthesis and Functionalization of a Mesoporous Silica Nanoparticle Based on the Sol–Gel Process and Applications in Controlled Release, Acc. Chem. Res. 40 (2007) 846-853.

[20] M. Jafarzadeh, I.A. Rahman, C.S. Sipaut, Synthesis of silica nanoparticles by modified sol–gel process: the effect of mixing modes of the reactants and drying techniques, J. Sol-Gel Sci. Technol. 50 (2009) 328-336.

[21] P.K. Jal, M. Sudarshan, A. Saha, S. Patel, B.K. Mishra, Synthesis and characterization of nanosilica prepared by precipitation method, Colloids and Surfaces A: Physicochemical and Engineering Aspects 240 (2004) 173-178.

[22] T. Aubert, F. Grasset, S. Mornet, E. Duguet, O. Cador, S. Cordier, Y. Molard, V. Demange, M. Mortier, H. Haneda, Functional silica nanoparticles synthesized by water-in-oil microemulsion processes, J. Colloid Interface Sci. 341 (2010) 201-208.

[23] M.S. Wooldridge, P.V. Torek, M.T. Donovan, D.L. Hall, T.A. Miller, T.R. Palmer, C.R. Schrock, An experimental investigation of gas-phase combustion synthesis of SiO2 nanoparticles using a multi-element diffusion flame burner, Combust. Flame 131 (2002) 98-109.

[24] A.B. Corradi, F. Bondioli, A.M. Ferrari, B. Focher, C. Leonelli, Synthesis of silica nanoparticles in a continuous-flow microwave reactor, Powder Technol. 167 (2006) 45-48.

[25] X. Cai, R.Y. Hong, L.S. Wang, X.Y. Wang, H.Z. Li, Y. Zheng, D.G. Wei, Synthesis of silica powders by pressured carbonation, Chem. Eng. J. 151 (2009) 380-386.

[26] W. Stober, A. Fink, E. Bohn, Controlled growth of monodisperse silica spheres in micron size range., J. Colloid Interface Sci. 26 (1968) 62-69.

[27] T. Matsoukas, E. Gulari, Dynamics of growth of silica particles from ammonia-catalyzed hydrolysis of tetra-ethyl-orthosilicate, J. Colloid Interface Sci. 124 (1988) 252-261.

[28] National Center for Biotechnology Information. PubChem Compound Database; CID=18730, https://pubchem.ncbi.nlm.nih.gov/compound/18730.

[29] L. Wang, W. Zhao, W. Tan, Bioconjugated Silica Nanoparticles: Development and Applications, Nano Research 1 (2008) 99-115.

[30] A. Guerrero-Martinez, J. Perez-Juste, L.M. Liz-Marzan, Recent Progress on Silica Coating of Nanoparticles and Related Nanomaterials, Adv Mater 22 (2010) 1182-1195.

[31] S. Giri, B.G. Trewyn, V.S.Y. Lin, Mesoporous silica nanomaterial-based biotechnological and biomedical delivery systems, Nanomedicine 2 (2007) 99-111.

[32] A. Vanblaaderen, A. Vrij, Synthesis and Characterization of Colloidal Dispersions of Fluorescent, Monodisperse Silica Spheres, Langmuir 8 (1992) 2921-2931.

[33] S. Santra, B. Liesenfeld, C. Bertolino, D. Dutta, Z.H. Cao, W.H. Tan, B.M. Moudgil, R.A. Mericle, Fluorescence lifetime measurements to determine the core-shell nanostructure of FITC-doped silica nanoparticles: An optical approach to evaluate nanoparticle photostability, J. Lumin. 117 (2006) 75-82.

[34] L.M. Rossi, L.F. Shi, F.H. Quina, Z. Rosenzweig, Stober synthesis of monodispersed luminescent silica nanoparticles for bioanalytical assays, Langmuir 21 (2005) 4277-4280.

[35] W. Lian, S.A. Litherland, H. Badrane, W.H. Tan, D.H. Wu, H.V. Baker, P.A. Gulig, D.V. Lim, S.G. Jin, Ultrasensitive detection of biomolecules with fluorescent dye-doped nanoparticles, Anal. Biochem. 334 (2004) 135-144.

[36] A. Imhof, M. Megens, J.J. Engelberts, D.T.N. de Lang, R. Sprik, W.L. Vos, Spectroscopy of fluorescein (FITC) dyed colloidal silica spheres, J. Phys. Chem. B 103 (1999) 1408-1415.

[37] N. Zhang, E. Ding, X. Feng, Y. Xu, H. Cai, Synthesis, characterizations of dye-doped silica nanoparticles and their application in labeling cells, Colloids and Surfaces B-Biointerfaces 89 (2012) 133-138.

[38] S. Biffi, L. Petrizza, E. Rampazzo, R. Voltan, M. Sgarzi, C. Garrovo, L. Prodi, L. Andolfi, C. Agnoletto, G. Zauli, P. Secchiero, Multiple dye-doped NIR-emitting silica nanoparticles for both flow cytometry and in vivo imaging, Rsc Adv 4 (2014) 18278-18285.

[39] S. Santra, H. Yang, D. Dutta, J.T. Stanley, P.H. Holloway, W.H. Tan, B.M. Moudgil, R.A. Mericle, TAT conjugated, FITC doped silica nanoparticles for bioimaging applications, Chem. Commun. (2004) 2810-2811.

Table-1 Different molar ratios of precursors to synthesis the silica NPs

Sample	NH_3/ TEOS	NH_3/EtOH	Particle Size (nm)
SiN20	2.22	0.47	20
SiN52	3.55	0.75	52
SiN95	4.69	0.99	95
SiN210	7.92	1.15	210
SiN410	8.86	1.68	410

Table-2 BET Surface Area, BJH Pore Volume and Pore diameter of each product

Sample	NH_3/ TEOS	BET surface area ($m^2\ g^{-1}$)	BJH pore volume ($cm^3\ g^{-1}$)	Pore diameter (Å)
SiN20	2.22	101 (114)	0.30	120
SiN52	3.55	64 (43)	0.13	96
SiN95	4.69	31 (24)	0.05	85
SiN210	7.92	8 (10.8)	0.01	77
SiN410	8.86	5 (5.5)	0.003	72

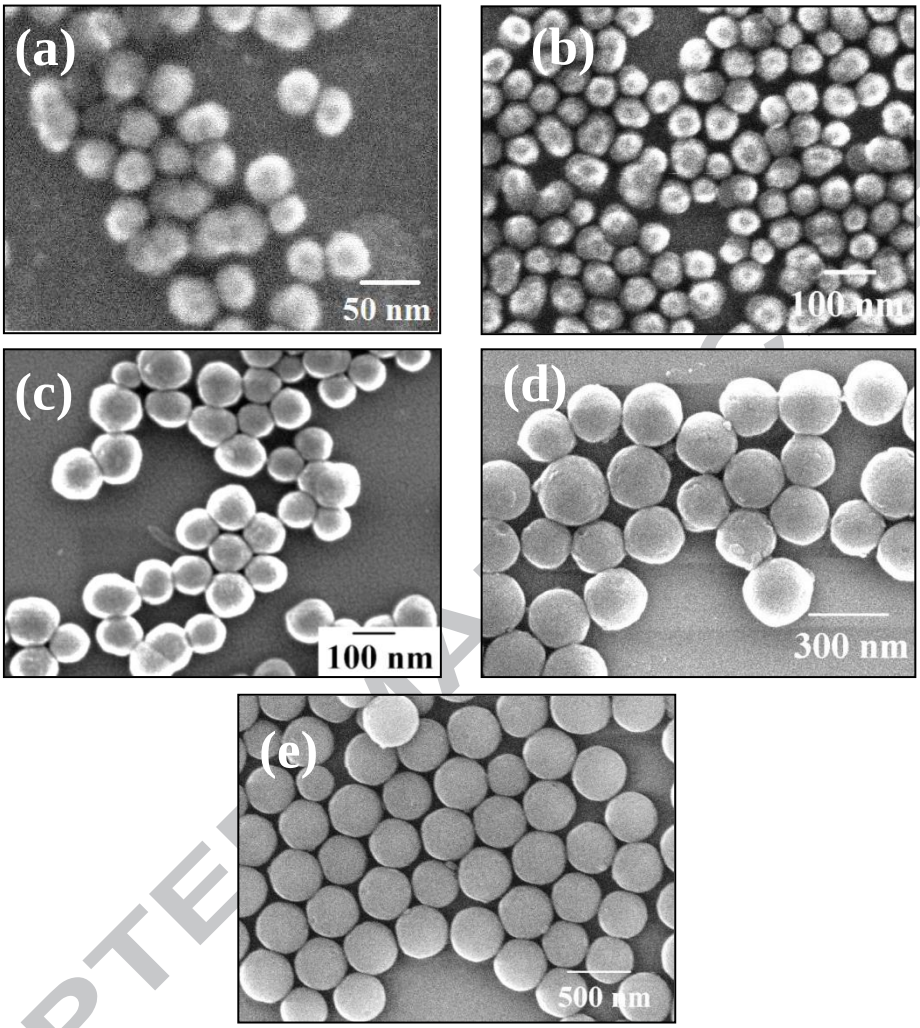

Fig. 1. SEM images of silica NPs (a) SiN20 (b) SiN52 (c) SiN95 (d) SiN210 and (e) SiN410.

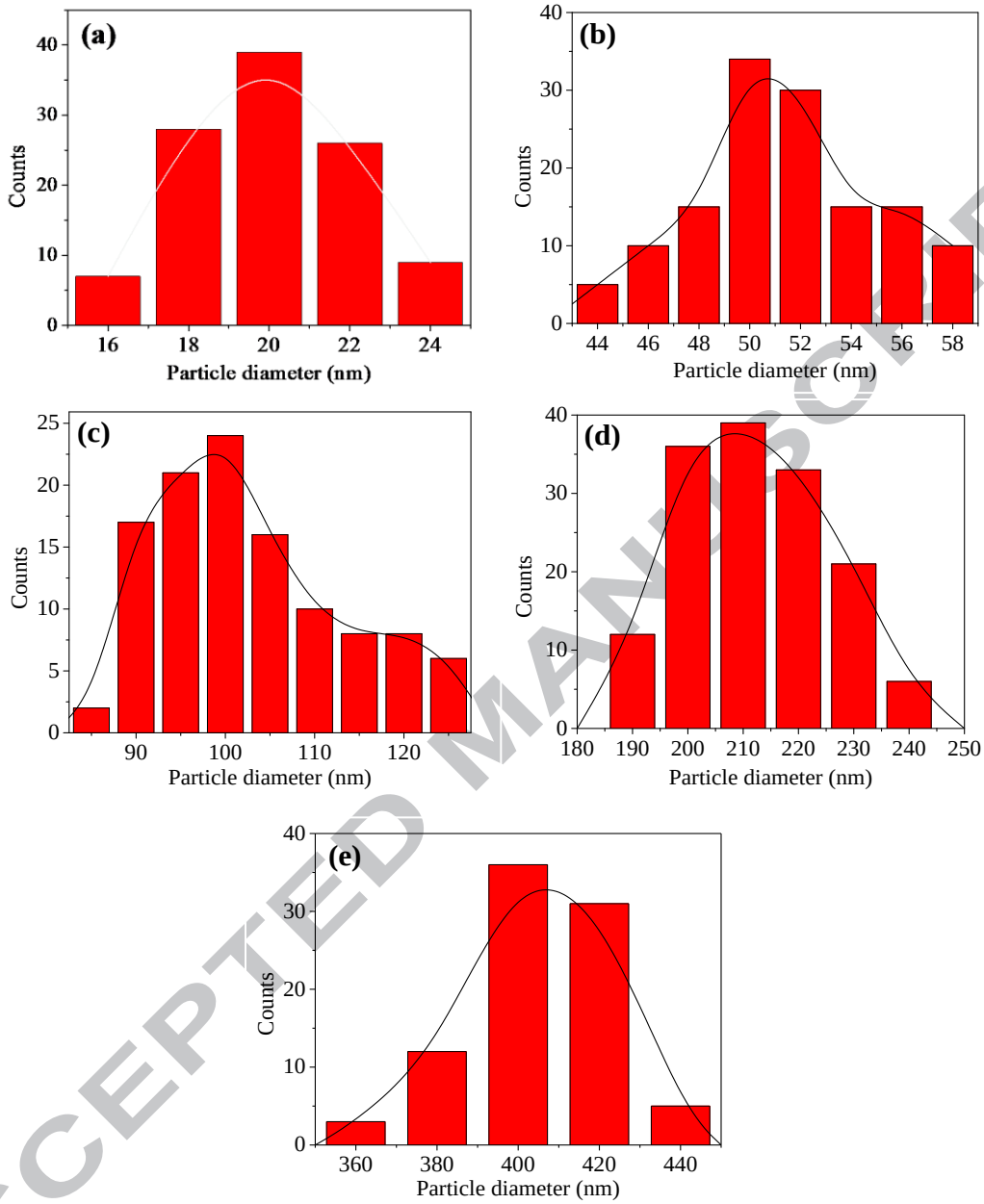

Fig. 2. Particle size distribution of silica NPs (a) SiN20 (b) SiN52 (c) SiN95 (d) SiN210 and (e) SiN410.

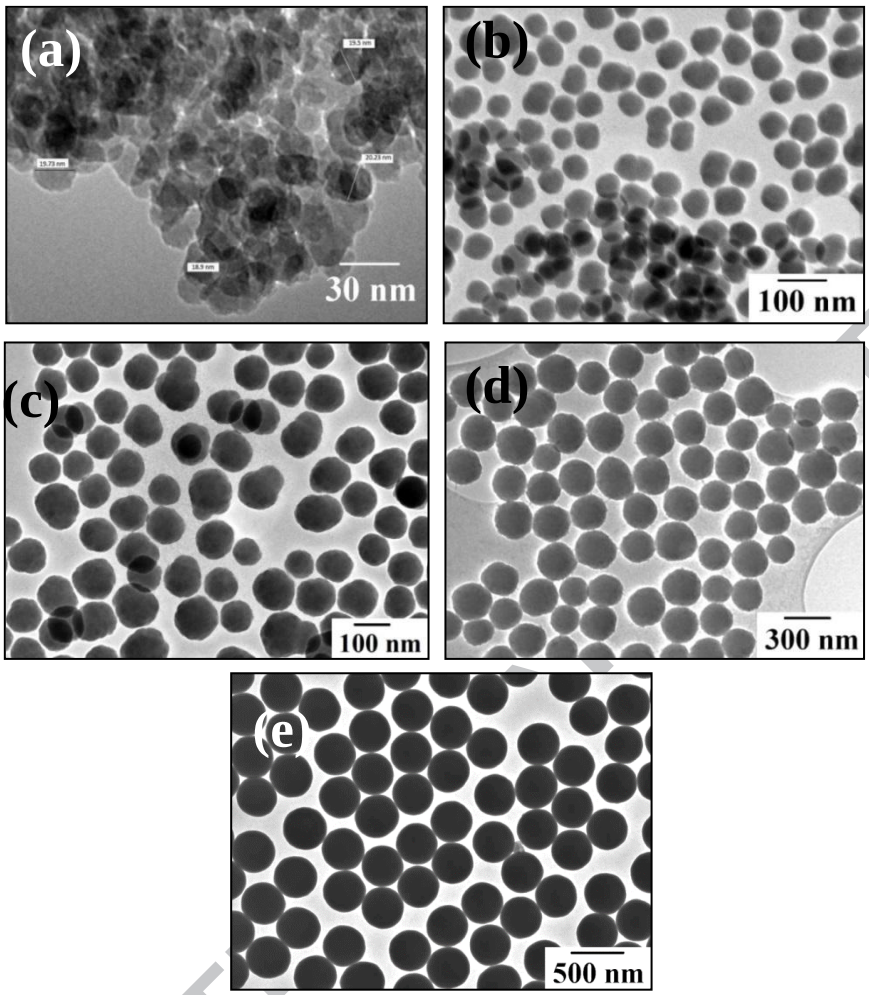

Fig. 3. TEM images of the silica NPs (a) SiN20 (b) SiN52 (c) SiN95 (d) SiN210 and (e) SiN410.

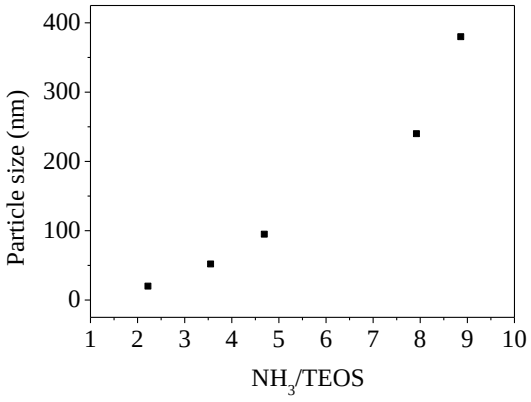

Fig. 4. Plot of particle size vs the NH_3/TEOS ratio.

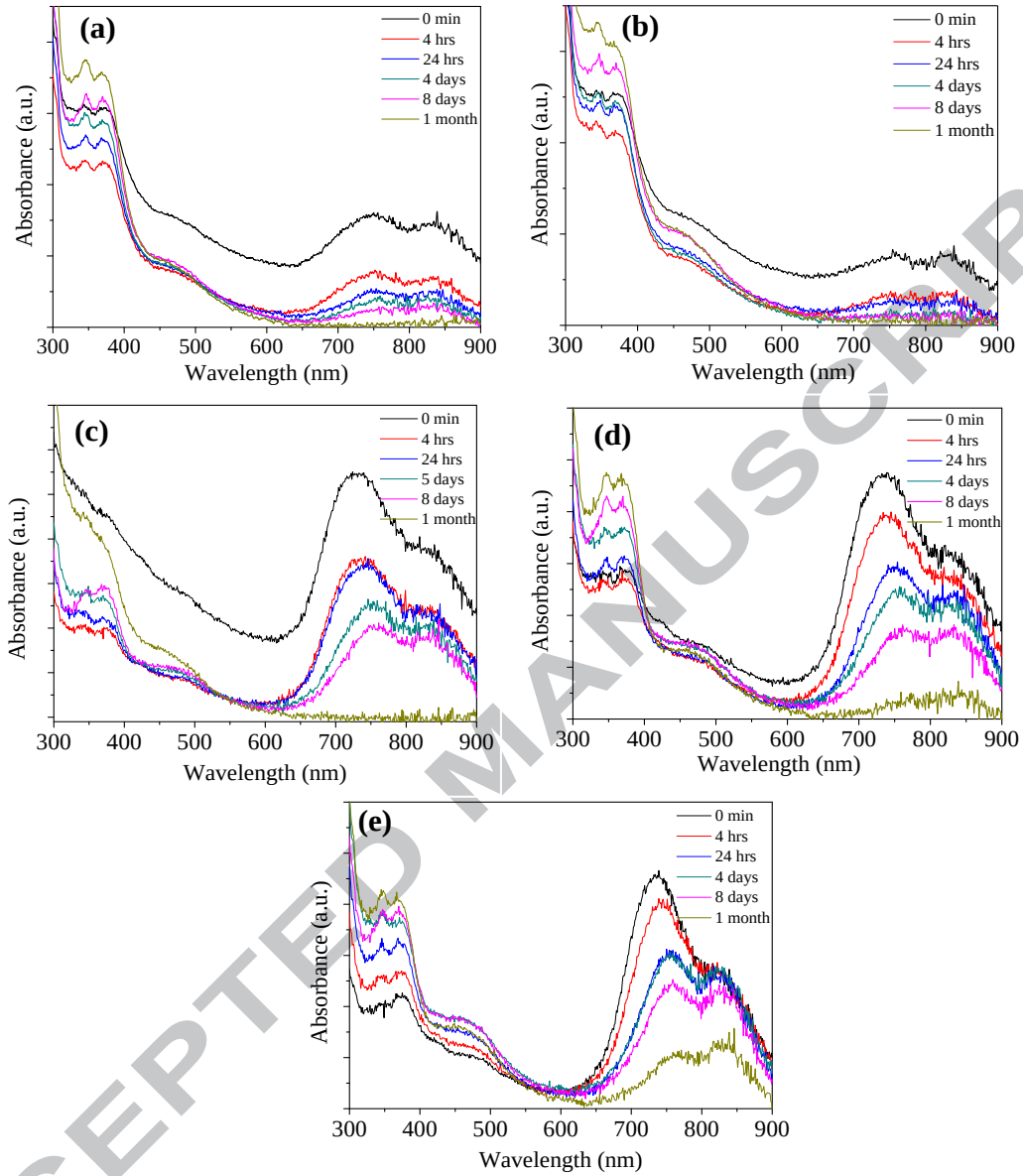

Fig. 5. UV-Vis absorbance spectra of IR-820 dye-doped silica NPs (a) SiN20 (b) SiN52 (c) SiN95 (d) SiN210 and (e) SiN410 with different aging time.

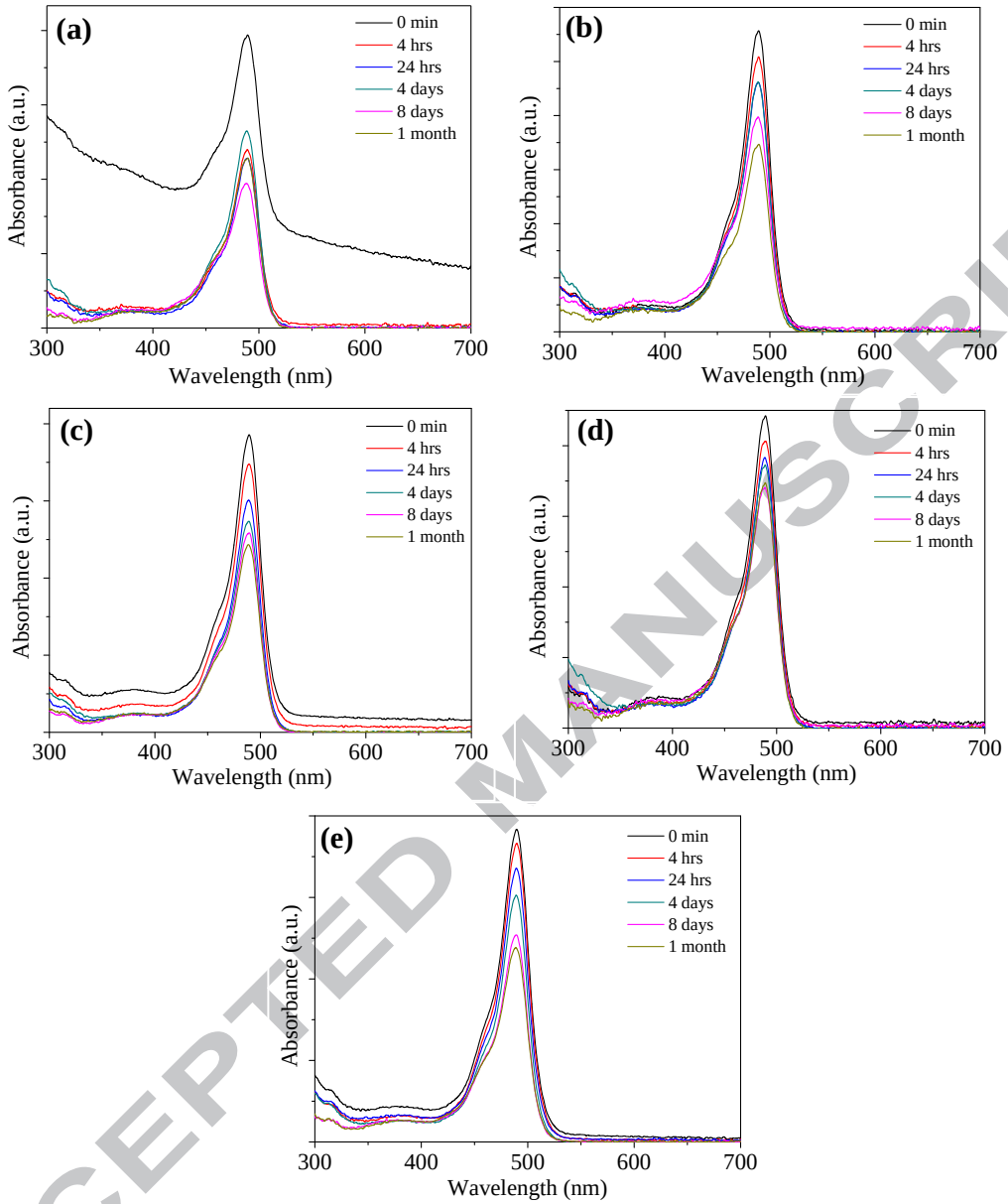

Fig. 6. UV-Vis absorbance spectra of FITC dye-doped silica NPs (a) SiN20 (b) SiN52 (c) SiN95 (d) SiN210 and (e) SiN410 silica NPs with different aging time.

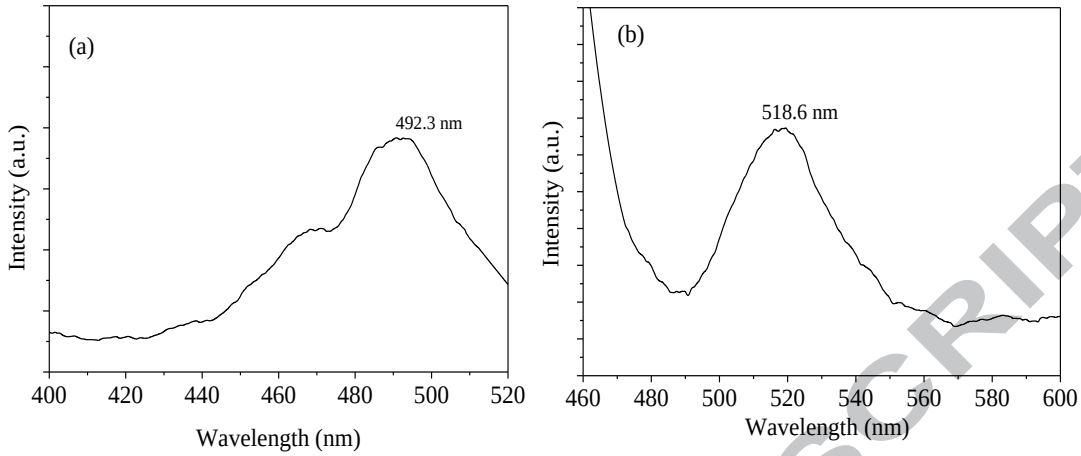

Fig. 7. (a) Excitation spectra of FITC doped silica NPs (SiN95). Emission wavelength was 520 nm (b) Emission spectra of FITC doped silica NPs (SiN95). The excitation wavelength was 450 nm.

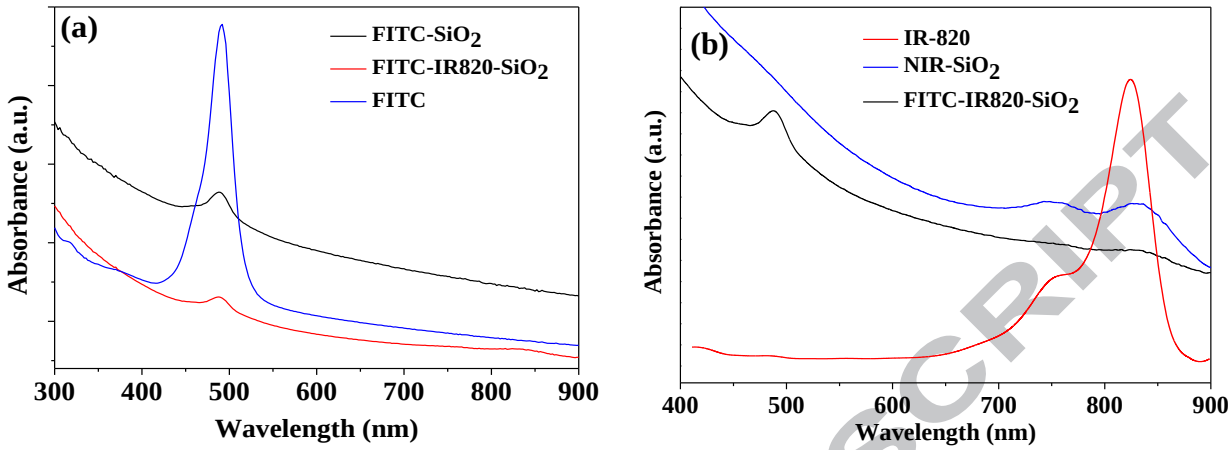

Fig. 8: UV-Vis absorbance spectra of (a) FITC dye, dye conjugate and dual dye-doped silica nanoparticles (SiN95). (b) IR-820 dye, dye conjugate and dual dye-doped silica nanoparticles (SiN95).

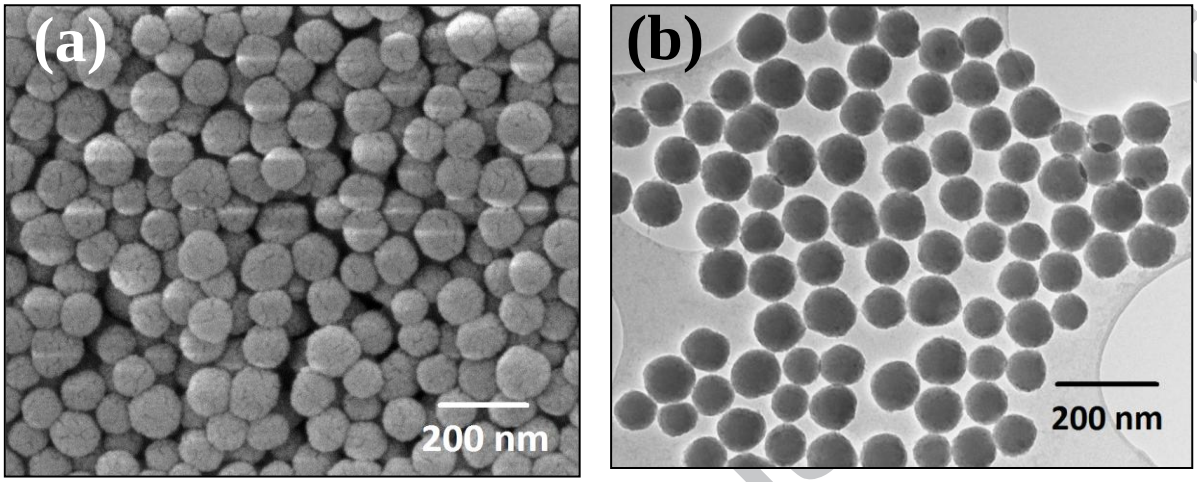

Fig. 9: (a) SEM image of dual dye-doped silica nanoparticles (b) TEM image of duel dye-doped silica nanoparticles.

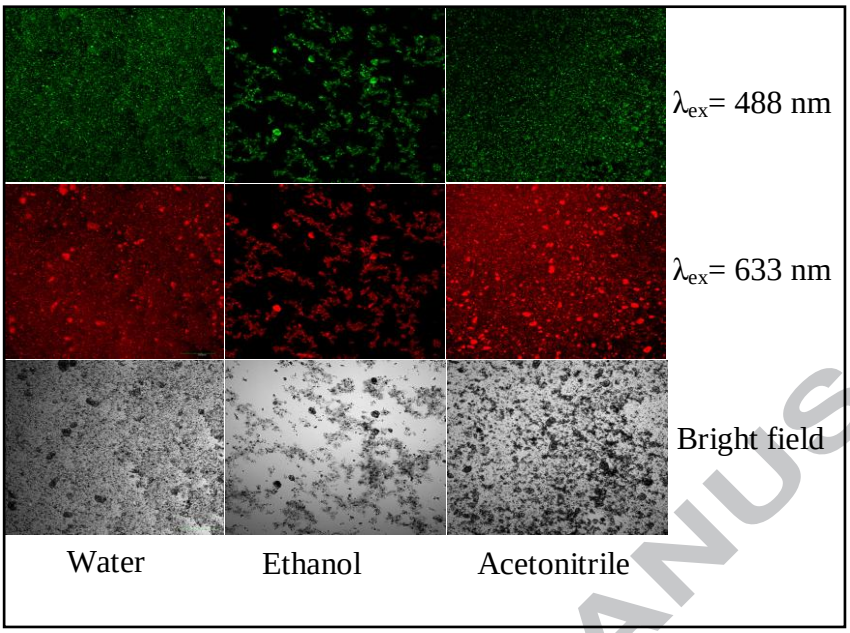

Fig. 10. Confocal laser scanning microscope images of FITC-IR820-SiO_2 NPs.

*3: Graphical Abstract